Development 137, 1385-1394 (2010) doi:10.1242/dev.048520

Actomyosin contractility and Discs large contribute to junctional conversion in guiding cell alignment within the *Drosophila* embryonic epithelium

Robert P. Simone and Stephen DiNardo*

SUMMARY

Proper control of epithelial morphogenesis is vital to development and is often disrupted in disease. After germ band extension, the cells of the *Drosophila* ventral embryonic epidermis are packed in a two-dimensional polygonal array. Although epithelial cell rearrangements are being studied productively in several tissues, the ventral epidermis is of particular interest as the final cell arrangement is, uniquely, far from equilibrium. We show that over the course of several hours, a subset of cells within each parasegment adopts a rectilinear configuration and aligns into parallel columns. Live imaging shows that this is accomplished by the shrinkage of select cell interfaces, as three-cell junctions are converted to four-cell junctions. Additionally, we show that non-muscle Myosin II and the polarity proteins Discs large (Dlg) and Bazooka are enriched along cell interfaces in a complex but reproducible pattern that suggests their involvement in junctional conversion and cell alignment. Indeed, depletion of Myosin II or *dlg* disrupts these processes. These results show that tight spatial regulation of actomyosin contractility is required to produce this high-energy arrangement of cells.

KEY WORDS: Discs large (Dlg; Dlg1), Bazooka (Baz; Par3), *Drosophila*, Morphogenesis, Myosin II

INTRODUCTION

Cells within an epithelium will tend to pack closely together, adopting roughly polygonal contours to maximize cell-cell contacts and thus minimize energy expenditure (Lecuit and Lenne, 2007). However, in most tissues, function often dictates that cells pack into arrangements that are far from equilibrium. Active cell-biological mechanisms must be engaged for cells to adopt such configurations, and these processes must be under the control of developmental signals. Thus, understanding tissue morphogenesis requires uncovering the cell biology involved, and ultimately coupling that understanding with the initiating developmental signals. A number of morphogenetic events are being studied intensively with this purpose, including convergence and extension, which drives body axis elongation (Bertet et al., 2004; Blankenship et al., 2006; da Silva and Vincent, 2007; Heisenberg et al., 2000; Irvine and Wieschaus, 1994; Keller, 2002; Wallingford et al., 2000) and, in *Drosophila*, epithelial packing among wing and retinal cells (Adler, 2002; Classen et al., 2005; Hayashi and Carthew, 2004).

These morphogenetic events cover relatively large areas, requiring that all cells in a tissue be given the same instructions in order to intercalate or segregate. Thus, the principles being studied must guide wholesale cell shape change. However, in many tissues, cells must form intricate patterns, such as the arrangement of sensory and support cells in the vertebrate inner ear (McKenzie et al., 2004; Tilney and Saunders, 1983). In such cases, many different cell shapes must be coordinated precisely, simultaneously and independently to give rise to functional tissue. The degree to which such complexity of pattern might be explained by principles that apply over the large scale is unclear. Here, we use the *Drosophila* embryo to describe the fine-scale and complex process of cell column alignment.

During embryogenesis, subsets of cells across each abdominal parasegment produce actin-based protrusions called denticles that become extensions of the cuticle. There are seven columns of cells that contribute to the denticle field, and two types of patterning event that act across this field. First, the actin-based protrusions that template the cuticle pattern emanate only from the posterior edge of prospective denticle field cells (Dickinson and Thatcher, 1997; Price et al., 2006; Walters et al., 2006). Secondly, each cell aligns its anterior and posterior edges with the cells located dorsally and ventrally to it, thus forming parallel columns (Walters et al., 2006). In contrast to close-packed hexagonal cells at low-energy expenditure, parallel cell columns contain rectangular cells in a high-energy arrangement (Lecuit and Lenne, 2007). Together, these two patterning events produce precisely aligned, parallel columns of denticles that are necessary for efficient motility.

Of these two phenomena, the placement of actin-based protrusions at cell edges has been studied most intensively in developing wing hair cells (reviewed by Adler, 2002; Wong and Adler, 1993). Recently, there has been increased focus on how cells change shape, but very little is known about how cells align into parallel columns or into similar precise patterns. Much of what is known about the mechanics of cell shape change comes from studies of *Drosophila* convergent extension (CE), which is the process by which the body axis is elongated by a combination of low- and high-order neighbor exchange and directional cell division (Bertet et al., 2009; Bertet et al., 2004; da Silva and Vincent, 2007; Fernandez-Gonzalez et al., 2009; Irvine and Wieschaus, 1994; Zallen and Wieschaus, 2004). In one model, cells exchange neighbors by converting three-cell junctions to four-cell junctions, and then back to orthogonally oriented three-cell junctions. These conversions result in the interdigitation of neighboring rows of cells, leading to tissue elongation.

University of Pennsylvania Medical School, Department of Cell and Developmental Biology, 421 Curie Boulevard, Philadelphia, PA 19104-6048, USA.

*Author for correspondence (sdinardo@mail.med.upenn.edu)

Accepted 11 February 2010

Junctional conversions during CE require non-muscle Myosin II contractility (Bertet et al., 2009; Bertet et al., 2004; Fernandez-Gonzalez et al., 2009). Myosin II is a heterohexamer composed of two ATP-hydrolyzing heavy chains, two regulatory light chains and two essential light chains. During CE, through mechanisms that are not well understood, Myosin II is required for the elimination of three-cell junctions and the formation of four-cell junctions. After the formation of four-cell junctions, three-cell junctions re-emerge but the new junction is invariably positioned orthogonally to the originally three-cell junction. Although there are a number of extant questions concerning CE, it is clear that some form of global control marks anteroposterior (AP) cell contacts as distinct from dorsoventral (DV) contacts (Bertet et al., 2004; Irvine and Wieschaus, 1994; Zallen and Wieschaus, 2004). Only AP contacts (that participate in three-cell junctions) are enriched for Myosin II and are eliminated, and only newly forming DV contacts are stabilized to resolve four-cell junctions back into three-cell junctions. In this manner, cell intercalation over the bulk of the embryo is coordinated and the body axis elongates.

The mechanism that leads to Myosin II enrichment along shrinking contacts during CE is unknown. In many instances, cell membranes are partitioned into distinct domains by conserved protein complexes. For example, in epithelia, the Crumbs (Crb), Bazooka (Baz, also known as Par3) and Discs large (Dlg, also known as Dlg1) complexes cooperate to form three distinct subcellular membrane domains along the apical basal cell axis (Bilder et al., 2000; Hutterer et al., 2004; Tanentzapf and Tepass, 2003; Wodarz et al., 1995; Yamanaka et al., 2003). These complexes maintain unique membrane domains by antagonizing the activity of each other through mutual inhibition, similar to how the Partitioning defective (Par) proteins act in the *C. elegans* zygote (Kemphues et al., 1988). Interestingly, during CE, Baz is enriched in a domain reciprocal to that of Myosin II, as Baz is depleted from shrinking three-cell junctions and is enriched on the orthogonal, newly forming junctions (Zallen and Wieschaus, 2004). Surprisingly, mutual antagonism is not responsible for these complementary enrichments, as compromising the function of the Baz polarity complex does not affect Myosin II enrichment (Blankenship et al., 2006).

Here, we show that epithelial cells align their AP boundaries and adopt a parallel column arrangement that is far from equilibrium. Junctional conversion occurs during this process, and it initiates in a position-specific manner within each parasegment. We describe complementary enrichments of actomyosin and various polarity proteins, and this is likely to contribute to the selectivity in junctional conversion. Finally, as only a specific subset of cells within each parasegment aligns, this tissue presents a novel paradigm to study the finer-scale cellular arrangements within an epithelium.

MATERIALS AND METHODS

Fly stocks

Fly stocks used were: PtcGal4 UAS-GFP; Serrate-lacZ (Bachmann and Knust, 1998); P{sqh-Moe.GFP} (FBtp0012637) (Kiehart et al., 2000); ArmGal4 α-Catenin-GFP (Oda and Tsukita, 1999); Spaghetti squash-GFP (Royou et al., 2002); *ush*[2] (FBal0017649) (Frank and Rushlow, 1996). We first analyzed *zip*-depleted embryos that contained mosaic patches of *zip*-expressing tissue, marked by Zip-GFP, as an internal control (Franke et al., 2005). Such embryos were generated by the cross *zip*[1] e22c-Gal4/CyO × *zip*[2] UAS-Zip-GFP/CyO. *zip*-depleted embryos enhanced by Lgl expression were from the cross *zip*[1]/CyO Kr-Gal4 UAS-GFP; P{Lgl+}/P{Lgl+} × *zip*[2]/CyO Kr-Gal4 UAS-GFP; P{Lgl+}/P{Lgl+} (FBal0018862, FBal0018863) (Franke et al., 2005). Analysis of Dlg-deficient embryos was conducted as described (Perrimon, 1988). Dlg permissive embryos were collected from homozygous *dlg*[HF321] (FBal0002671) (Woods and Bryant, 1989) females kept at 29°C for 2 hours before egg laying and mated to homozygous males. Dlg non-permissive embryos were collected from homozygous *dlg*[HF321] females kept at 29°C for between 4 and 7 days before egg laying and mated to homozygous males. Relatively few embryos were recovered from females kept at 29°C for over 4 days, as reported previously (Perrimon, 1988).

Microscopy, fixation, cuticle preparations and immunofluorescence

Embryos were collected either overnight or for 2 hours and aged to the appropriate stage. Sqh-GFP embryos were fixed using 4% paraformaldehyde and heptane for 20 minutes, the Baz antibody was used on heat-fixed embryos (Miller et al., 1989), and all other embryos were fixed for 7 minutes in 37% paraformaldehyde and heptane. All embryos were devitellinized with methanol, except those stained with Rhodamine-coupled phalloidin. Embryos were processed to visualize cuticle pattern by phase-contrast microscopy (van der Meer, 1977). Images of fixed embryos were captured using a Zeiss microscope using structured (Apotome) illumination. Time-lapse images were acquired using a spinning disk confocal system (BioVision Technologies), built around an Olympus IX71 microscope, using an Olympus 100× 1.4 NA UPlanSApo lens and a CSU10 scanhead (Yokogawa), and controlled using IPLab software (BD Scientific).

Primary antibody incubations were overnight at 4°C and included: rabbit anti-GFP (1:2000, Molecular Probes), chicken anti-GFP (1:2000, Aves Labs), mouse anti-phosphotyrosine (1:2000, Upstate Cell Signaling), rabbit anti-β-galactosidase (1:2000, Molecular Probes), chicken anti-β-galactosidase (1:2000, Abcam), rabbit anti-Zipper (1:250) (Kiehart and Feghali, 1986), rat anti-DE-Cadherin [1:20, Developmental Studies Hybridoma Bank (DSHB)], rabbit anti-Baz (1:500) (Wodarz et al., 1999), mouse anti-Dlg (two different aliquots were used, one at 1:1000 and one at 1:20, DSHB), mouse anti-Crb (1:20, DSHB), mouse anti-aPKC (1:200, BioMol) and rabbit anti-Armadillo (Arm) (1:200, a gift from Eric Wieschaus, Princeton University). Rhodamine-coupled phalloidin was used at 1:200 (Molecular Probes).

Alignment and enrichment quantification

We measured the angle between each neighboring cell along a developing column at each of several stages (see Fig. S3A in the supplementary material). The average alignment was derived by scoring one parasegment in each individual embryo, and ten individuals for each stage or condition, and values compared using Student's *t*-test. We plotted the data after converting angles to a percentage of an idealized, aligned column (100%).

Pixel quantification was performed using ImageJ (NIH). Average fold enrichment values were determined between individual embryos. Within individual embryos, fold enrichment was derived by measuring five contact pairs (i.e. a shrinking and neighboring stable contact) for fold enrichment and averaging those values. Standard deviation is shown for each average value.

RESULTS

Denticle field cells align their anterior and posterior edges

We analyzed the progression of alignment as embryos age by examining apical cell outlines in fixed samples. Staining for the adherens junction marker DE-Cadherin (Shotgun – FlyBase) revealed that during stage 11, cells of the prospective denticle field were arranged as irregular polygons (Fig. 1A,A′). The AP boundaries of most cells were not in register along the DV axis (Fig. 1A,B, above and below). By stage 13, all cells within each parasegment had begun to elongate along the DV axis, increasing their axial ratio. Coincident with this global change in morphology, cells of the prospective denticle field began to align their AP edges with cells located above and below within the field (Fig. 1C,

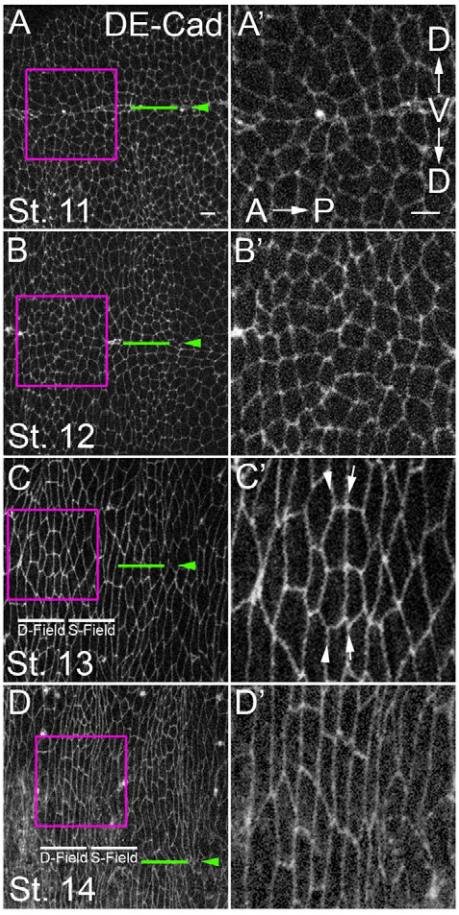

Fig. 1. Cells of the *Drosophila* ventral epidermis align their anterior and posterior edges over time.
(**A-D′**) Immunofluorescence staining of ventral epidermis for DE-Cadherin. Anterior is to left. Approximately two parasegments are visible in A-D and roughly one parasegment from each (boxed) is magnified in A′-D′. Green lines and arrowheads mark the ventral midline. D-field, denticle field; S-field, smooth field. Some boundaries align before others (C′, compare arrows with arrowheads). The ellipse-shaped cell contours along the midline in A and B are the last signs of the ventral seam stitching up (Martinez Arias, 1993). Scale bars: 5 μm.

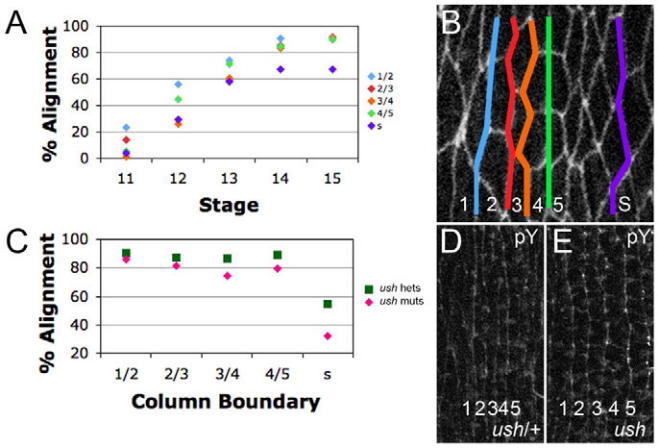

Fig. 2. The 1/2 and 4/5 boundaries align before their neighbors and *ush* mutants align normally. (**A**) Alignment by stage. (**B**) Stage 13 denticle field with columns marked by number and column boundaries marked by color. At stages 12 and 13, the 1/2 and 4/5 boundaries are significantly better aligned than the 2/3, 3/4 and smooth boundaries. At stages 14 and 15, all columns of the denticle field are significantly better aligned than the smooth field boundary. (**C**) Alignment by column, comparing *ush* mutants (muts) with *ush* heterozygotes (hets). (**D**,**E**) Anti-phosphotyrosine (pY)-stained embryos. Denticle field alignment is nearly identical in homozygous *ush* mutants (E) and *ush*/+ (D).

arrows). By stage 14, prospective denticle field cells had completely aligned their AP edges, forming parallel columns, whereas cells of the smooth field were not aligned to the same degree (see Fig. 2A).

Alignment did not progress evenly along all AP boundaries and some aligned before their neighbors (Fig. 1C′, compare arrows with arrowheads). To determine which interfaces aligned first, we measured the alignment over time of each boundary within the prospective denticle field, and compared this with a position within the smooth field (see Materials and methods). As expected, at stage 11, all boundaries were largely unaligned (Fig. 2A). By stage 12, all boundaries had become better aligned. However, the boundary between cell columns 1 and 2, and that between cell columns 4 and 5 (hereafter ‘1/2’ and ‘4/5’, respectively), exhibited significantly (P<0.005) more alignment than the neighboring 2/3 and 3/4 boundaries or a smooth field boundary (Fig. 2A). Although overall alignment again increased by stage 13, the 1/2 and 4/5 boundaries were still better aligned than those of their neighbors. By stage 14, all columns of the denticle field were equivalently aligned, and each of these was better aligned than the representative smooth field boundary.

These data raised two issues. First, as there was prominent cell elongation during this period, did elongation contribute to alignment? Second, as the 1/2 and 4/5 boundaries aligned first, what cell-biological changes occurred along these interfaces?

Cell stretching contributes little to denticle field alignment

After germband retraction, dorsal closure stretches the epidermis, increasing the axial ratio of cells (Schock and Perrimon, 2002). *u-shaped* (*ush*) mutants fail to retract completely and do not initiate dorsal closure, but otherwise complete embryogenesis (Nüsslein-Volhard et al., 1984). We measured the relative alignment of cells along each developing column across the prospective denticle field and also at one position within the prospective smooth field by measuring the angle between a given cell and the neighbors positioned immediately above and below it along a developing column (see Fig. S3A in the supplementary material). This was reiterated for several cells along each column and for each stage, and then expressed as a percentage alignment by comparing it with an idealized aligned column (100%). In *ush* mutants, smooth field cells did not align at all compared with sibling controls (Fig. 2C). Thus, for the smooth field, stretching along the DV axis makes a major contribution to alignment. By contrast, denticle field cells were still significantly aligned in *ush* mutants when compared with controls (Fig. 2C, and compare 2D with 2E), even though they were significantly less elongated (5±0.5 μm versus 8±0.75 μm). Thus, much of alignment derives from properties of the denticle field other than cell elongation.

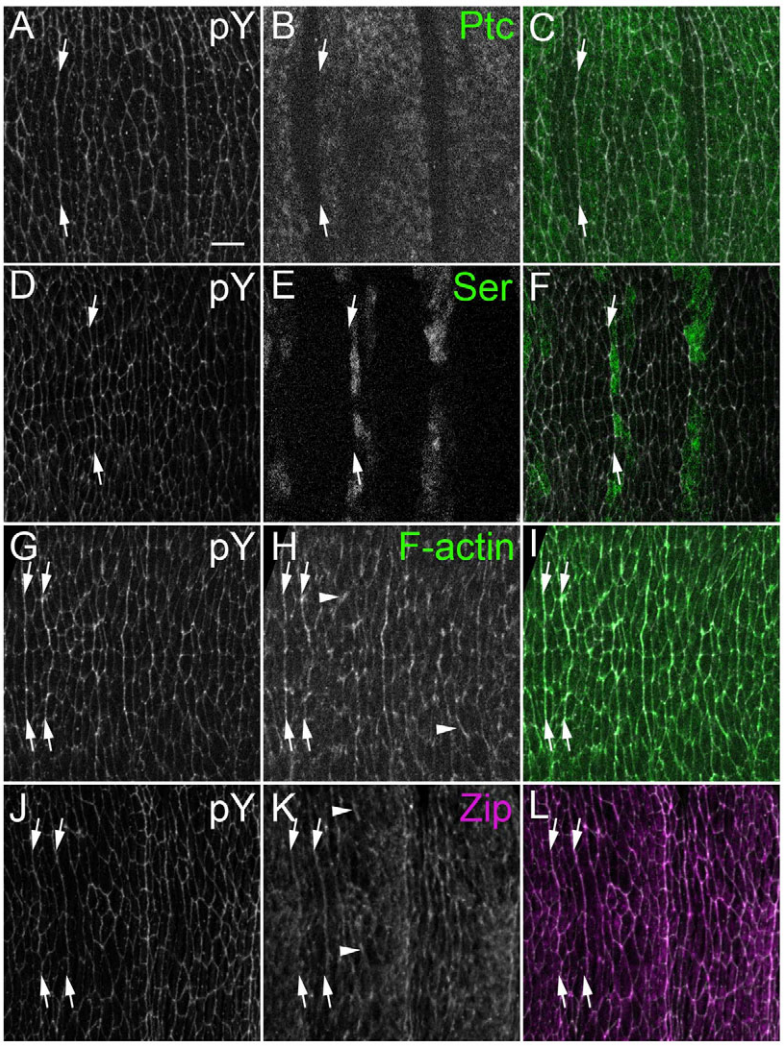

Fig. 3. pY, F-actin and Zip are enriched along the column 1/2 and 4/5 boundaries. Immunofluorescence for pY, Patched (Ptc), Serrate (Ser), F-actin and Zip. Anterior is to the left. Roughly two parasegments are visible. (**A-C**) PtcGal4 UAS-GFP embryos stained for (A) pY and (B) GFP (C, merge; GFP, green). Arrows mark pY enrichments at the 1/2 boundary between Ptc-expressing and non-expressing cells. (**D-F**) Ser-*lacZ*-expressing embryos stained for (D) pY and (E) for β-galactosidase by antibody (F, merge; *lacZ*, green). Arrows mark pY enrichments at the 4/5 boundary between Ser-expressing and non-expressing cells. (**G-I**) P{sqh-Moe.GFP}-expressing embryos stained for (G) pY and (H) GFP (I, merge; GFP, green). Arrows mark pY and F-actin enrichments at the 1/2 and 4/5 boundaries. Arrowheads mark occasional, variably positioned enrichments. (**J-L**) Embryos stained for (J) pY and (K) Zip (L, merge; Zip, magenta). Arrows mark pY and Zip enrichments at the 1/2 and 4/5 boundaries. Arrowheads mark occasional, variably positioned enrichments. Scale bar: 5 μm.

F-actin and Myosin II are enriched along specific column boundaries

To begin to investigate how this non-equilibrium state of cell packing arises, we first examined the localization of a number of adherens junction-associated proteins and epitopes, such as phosphotyrosine (pY; which highlights cell outlines), Myosin II and filamentous actin (F-actin). For each of these epitopes, at each stage examined, there were occasional enrichments at cell interfaces that were not repeated within each parasegment (Fig. 3H, arrowheads). This is not surprising, given the central role such proteins play in cellular morphogenesis. In addition to these irregular enrichments, patterned enrichments were also detectable (Fig. 3, arrows) and appeared consistently along certain boundaries. This was particularly apparent in whole-embryo views (see Fig. S1 in the supplementary material). We mapped the enrichment positions relative to known gene expression patterns, and found that pY was enriched at the 1/2 boundary (Fig. 3A-C, arrows) and also at the 4/5 boundary (Fig. 3D-F, arrows). Enrichment became apparent at stage 12, as AP edges were aligning, and persisted at least until stage 15, after they had aligned (Fig. 3A-F; data not shown). pY, F-actin (Fig. 3G-I, arrows) and Myosin II (Fig. 3J-L, arrows; see also Fig. 6D) exhibited enrichment along the 1/2 and 4/5 boundaries, as well as at other interfaces that were not patterned (see Fig. S1 in the supplementary material). These position-specific enrichments singled out the incipient 1/2 and 4/5 interfaces for further analysis.

The 1/2 and 4/5 boundaries align by three- to four-cell junctional conversion

To investigate how the boundaries align, we imaged live embryos expressing α-Catenin-GFP (see Movies 1 and 2 in the supplementary material). In the description that follows, we refer to stills from these movies as well as color-coded tracings of cell outlines (Fig. 4; see Fig. 7). Since we found that the 1/2 and 4/5 boundaries behaved similarly, we present data from either interface in subsequent figures.

Before alignment, cells along the 1/2 and 4/5 boundaries met at three-cell junctions. We found that one consequence of the alignment process was that two such three-cell junctions were resolved into a single four-cell junction. To follow this, note that at the onset of the process, several three-cell junctions are visible in Fig. 7A and two are traced in Fig. 7B. In the first tracing, a cell from column 5 shared interfaces with two column 4 cells. The contacts along this three-cell junction formed a Y-shaped interface. The right and left panels of Fig. 7C highlight each of two adjacent Y-interfaces.

Live imaging demonstrated that one arm of each Y-shaped interface behaved differently from the others during alignment. Before alignment, two of the three arms ran along the 4/5 boundary (Fig. 4A, magenta and orange) and the third arm formed a contact between cells within the same column (Fig. 4A, green). During alignment, the magenta contact shrank (hereafter, the

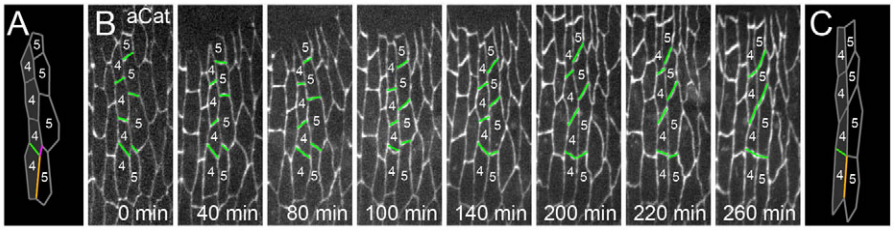

Fig. 4. The 1/2 and 4/5 boundaries align by directed cell contact shrinkage. (**A**,**C**) Schematics of the 0-minute (A) and 260-minute (C) timepoints in B. (**B**) Live recordings from an embryo expressing α-Catenin-GFP showing aligning denticle field cells along a 4/5 boundary. A boundary is brought into alignment by the conversion of two three-cell junctions to a four-cell junction and the elimination of the magenta contact highlighted in A.

'shrinking contact'). This led to the alignment of green contacts (hereafter, the 'stable contacts') from adjacent Y-interfaces (Fig. 4B). The selective elimination of the shrinking contact also brought the vertical orange contact (hereafter, the 'long contact') into alignment with its neighbor above (compare Fig. 4A and 4C; see also Fig. 7). Finally, the consequence of this all along the 1/2 boundary was to convert two three-cell junctions into one four-cell junction (compare Fig. 7B with 7H). Movie 2 starts at a slightly earlier timepoint than Movie 1 (see Movies 1 and 2 in the supplementary material), and the contribution of junctional conversion to alignment is more dramatic.

Myosin II is required for cell alignment

Previous work on CE identified a role for non-muscle Myosin II in the formation of four-cell junctions by the elimination of contacts between two three-cell junctions (Bertet et al., 2009; Bertet et al., 2004; Fernandez-Gonzalez et al., 2009). We examined embryos mutant for *zipper* (*zip*), which encodes the heavy chain of *Drosophila* Myosin II. Encouragingly, *zip* mutants exhibited disorganization of ventral pattern (see Fig. S2 in the supplementary material) (Walters et al., 2006). However, these phenotypes were exceedingly rare (1 in 25 mutant embryos). Such poor penetrance has been observed for dorsal closure defects by other laboratories, as maternally provided Zip complicates the analysis of zygotic *zip* mutants (Franke et al., 2005; Jacinto et al., 2002). To resolve the issue of maternal perdurance, the Kiehart laboratory exacerbated zygotic *zip* phenotypes by increasing the expression of a negative regulator of Zip, Lethal giant larvae [Lgl; L(2)gl – FlyBase] (Peng et al., 2000) (see Materials and methods). In that study, increased Lgl expression by itself had no effect on dorsal closure, but strongly exacerbated the dorsal closure phenotype of *zip* mutants in a dose-dependent manner.

Thus, we compared alignment between *zip* mutants and heterozygous siblings, both carrying two extra genomic copies of Lgl (hereafter, 4×Lgl). Using dorsal closure progression as a guide, we stage-matched embryos and focused on stage 13, at which the 1/2 and 4/5 boundaries are better aligned than their neighbors in wild type. Compared with heterozygous siblings, embryos from *zip* 4×Lgl mutants had significantly less alignment at the 1/2 and 4/5 boundaries, but not at the 2/3, 3/4 or smooth boundaries (Fig. 5A, and compare 5B with 5D). Embryos heterozygous for *zip*, but still 4×Lgl, exhibited no alignment defects (Fig. S3B in the supplementary material). Also, there was no significant difference (P=0.2) in cell elongation between *zip* 4×Lgl (8.16±1.05 μm) and heterozygous siblings (8.83±0.85 μm). This was consistent with our *ush* data, which demonstrated that elongation had little influence on alignment among denticle field cells. Thus, although we were unable to examine embryos completely deficient for Myosin II, all the evidence suggests that *zip*, and by extension actomyosin contractility, is required for cell alignment.

Myosin II is enriched along the shrinking and long contacts

Actomyosin contractility is regulated by Myosin II localization in a variety of contexts (Barros et al., 2003; Bertet et al., 2004; Wong et al., 2007). Since our data implicated actomyosin contractility in alignment, we tested whether Myosin II localization might be informative in understanding this process. We fixed and imaged embryos carrying a rescuing GFP fusion of the Myosin regulatory light chain, which is encoded by *spaghetti squash* (*sqh*) (Royou et al., 2002). At stage 11, before alignment, Sqh-GFP localized approximately uniformly around the cell cortex (Fig. 6A). Quantitation of pixel intensities showed little, if any, enrichment upon comparing the different DV cell edges (prospective shrinking versus stable contact, a fold difference of 1.22±0.21). The situation differed, however, by stage 13, when alignment was underway. Along the series of Y-shaped interfaces that make up the 1/2 and 4/5 boundaries, Sqh-GFP appeared to be enriched at shrinking (Fig. 6D, magenta arrow) as compared with stable (Fig. 6D, white arrows) contacts, and quantitation of pixel intensities supported this (fold difference of 2.09±0.4). Sqh-GFP was also enriched at the long contacts (Fig. 6D, magenta arrowhead). By contrast, along the contacts of column 3, the cells of which do not contribute to the 1/2 or 4/5 boundaries, Sqh-GFP displayed an irregular, but mostly uniform, localization (see Fig. S4A in the supplementary material, magenta asterisks). The column-specific and selective enrichments we observed are consistent with Myosin II acting at the shrinking contact to effect junctional conversion, as it does during CE. However, Myosin II enrichment on the long contact was unexpected, and will be discussed below.

Baz is enriched along the stable DV contact

Baz is often involved in establishing and maintaining specialized subcellular membrane domains. We examined Baz localization during alignment to see whether it could be involved in localizing Myosin II. At stage 11, before alignment, Baz was localized at the level of the adherens junction, and was only slightly enriched at prospective stable contacts over shrinking contacts (fold difference of 1.47±0.7) (Fig. 6B). By stage 13, Baz was still relatively uniformly localized along the contacts of cells making up the 2/3 and 3/4 boundaries (see Fig. S4B in the supplementary material, green asterisks). However, along the 1/2 and 4/5 boundaries at which alignment was underway, Baz accumulation appeared as 'rungs on a ladder' along the incipient 1/2 and 4/5 interfaces. This pattern was

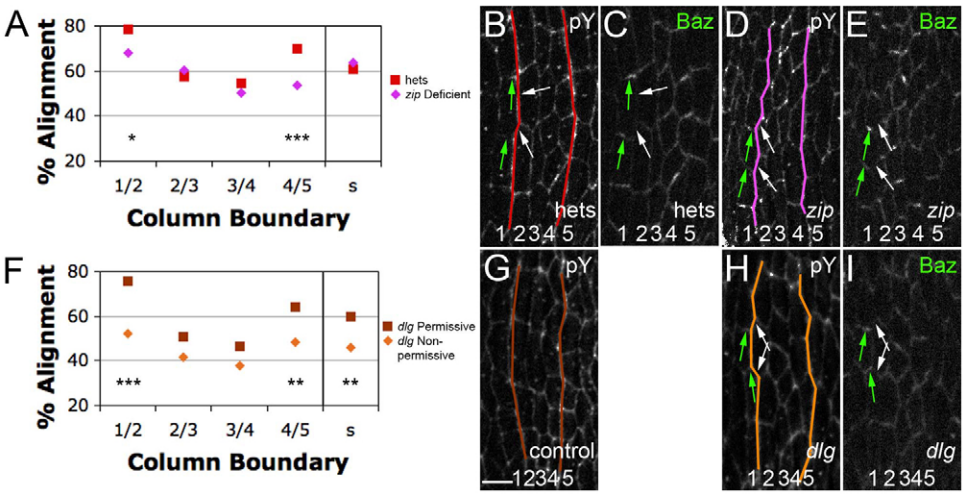

Fig. 5. *zip* and *dlg* are required for cell alignment. (A-I) Stage 13. (**A**) Alignment by column, comparing homozygous *zip* mutants (*zip* deficient) with heterozygotes (hets). All embryos express two extra genomic copies of *lgl*. (**B**,**D**) Anti-pY-stained embryos. The 1/2 and 4/5 boundaries (colored lines) are significantly less aligned in the mutants (D) compared with heterozygous siblings (B). (**C**,**E**) Baz is correctly localized in *zip*-deficient embryos (interface enrichments, green arrows; interface depletions, white arrows). (**F**) Alignment by column, comparing *dlg* mutants under permissive and non-permissive conditions. (**G**,**H**) Anti-pY-stained embryos. The 1/2, 4/5 and smooth boundaries are significantly less aligned (colored lines) in non-permissive conditions (H) than in permissive conditions (G). (**I**) Baz is correctly localized in *dlg*-deficient embryos. *, $P<0.05$; **, $P<0.005$; ***, $P<0.0005$. Scale bar: 5 μm.

due to Baz enrichment along the stable DV contacts (Fig. 6E, green arrows) as compared with the shrinking contacts (Fig. 6E, white arrow) (fold difference of 2.67±0.31). Baz was also relatively depleted from the long, stable contacts (Fig. 6E, white arrowhead). Unfortunately, we could not test whether Baz accumulation was important for stability of the DV contact because the epithelium of zygotic mutants was too disrupted to be informative. In addition, whereas Baz was relatively depleted from those interfaces that accumulated Myosin II (compare Fig. 6D with 6E), the Baz pattern did not change in *zip*-depleted embryos (Fig. 5E).

Dlg is enriched along the long contact

In many epithelia, Baz is involved in establishing and maintaining apical-basal epithelial polarity (Benton and Johnston, 2003; Tanentzapf and Tepass, 2003). Since it was enriched along only certain cell contacts during alignment, we tested other apical-basal regulatory proteins, including atypical Protein kinase C (aPKC) and Crb, that often localize to complementary membrane domains. We found aPKC to be enriched at stable contacts, but only during late stages of alignment (see Fig. S4E,K in the supplementary material). Crb levels were increased in prospective denticle as compared with smooth field cells (see Fig. S4O in the supplementary material), but were evenly distributed along all cell contacts (see Fig. S4F,L in the supplementary material).

Dlg exhibited the most interesting localization pattern. Before alignment, at stage 11, Dlg was localized relatively uniformly around the cortex, exhibiting similar levels on long contacts and shrinking contacts (Fig. 6C) (fold difference of 0.87±0.06). By stage 13, Dlg was still uniformly localized along the contacts of cells making up column 3, which contribute no interfaces to the 1/2 or 4/5 boundaries (see Fig. S4C in the supplementary material, orange asterisks). However, along the 1/2 and 4/5 boundaries at which alignment was underway, Dlg was enriched at long contacts (Fig. 6F orange arrows) as compared with the stable DV or shrinking contacts (Fig. 6F, white arrows) (fold difference of 1.6±0.17). This localization was intriguing because it suggested a molecular difference between the long and the shrinking contacts, both of which exhibited enrichment of Myosin II. Whereas one of the contacts enriched for Myosin II shrank, the other did not, and this was the contact enriched for Dlg. We thus hypothesized that Dlg was directly or indirectly counteracting Myosin II activity at long contacts.

Dlg is required for cell alignment

To test whether *dlg* was required for alignment, we had to circumvent the early requirements for Dlg during the initial establishment of apical-basal polarity at cellularization. To accomplish this, we used the temperature-sensitive hypomorphic allele *dlg*[HF231] (see Materials and methods).

We compared boundary straightness in *dlg*[HF321] embryos laid by adults kept at permissive conditions with that in embryos laid by adults kept under non-permissive conditions. Under non-permissive conditions, embryos exhibited significantly less alignment at their 1/2 and 4/5 boundaries, as well as at a smooth field boundary (Fig. 5F). Whereas Baz and Dlg were enriched along distinct cell interfaces, we found no alteration in Baz enrichment in embryos depleted for Dlg activity (Fig. 5I). Finally, we found no significant difference ($P=0.4$) upon comparing cell elongation between permissive (7.66±1.38 μm) and non-permissive (8.1±1.16 μm) conditions, consistent with our data indicating that elongation has little influence on alignment among denticle field cells. Thus, *dlg* is required for cell alignment but not for Baz enrichment. These observations are consistent with Dlg directly or indirectly interfering with Myosin II action on the long contacts on which Dlg is enriched during alignment.

DISCUSSION

Cell arrangement is intimately tied to tissue function, and the varied patterns that one observes argue that the mechanisms by which cells adopt such arrangements will also be varied. In the ventral epidermis

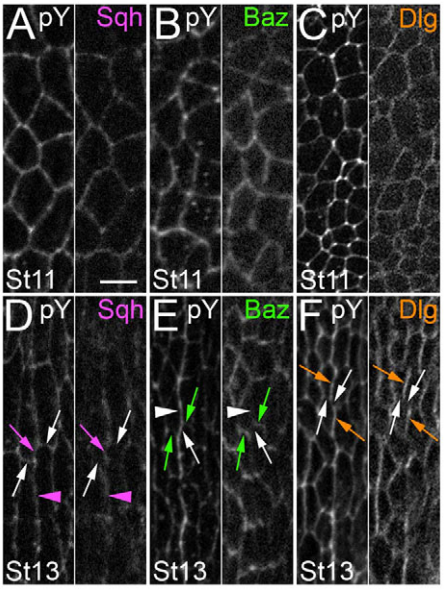

Fig. 6. Sqh, Baz and Dlg localization before and during alignment. Paired images. Cell outlines are highlighted by pY double labeling (the left of each pair). Anterior is to left. (**A-C**) Stage 11. Relatively uniform Sqh, Baz and Dlg localization. (**D-F**) Stage 13. (D) Sqh was enriched at shrinking (magenta arrow) and long (magenta arrowhead) contacts, and relatively depleted from the stable contacts (white arrows). (E) Baz was enriched at stable contacts (green arrows) and relatively depleted from the long and shrinking contacts (white arrow and arrowhead, respectively). (F) Dlg was enriched at the long contacts (orange arrows) and relatively depleted from the stable and shrinking contacts (white arrows). Scale bar: 5 μm.

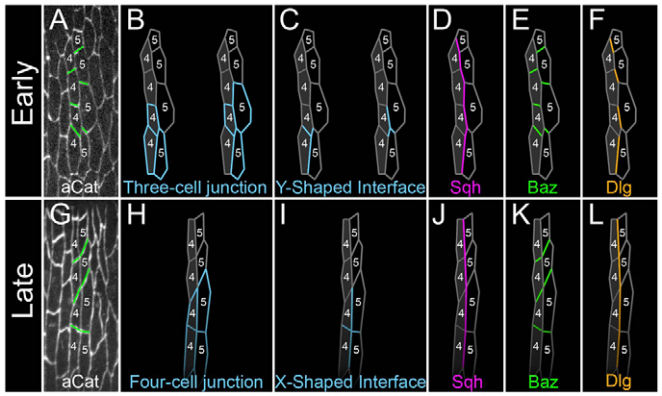

Fig. 7. Model for conversion of three- to four-cell junctions by *zip* and *dlg*. (**A**,**G**) Stills from a live recording of boundary alignment as followed by α-Catenin (aCat) staining. (**B-F**,**H-L**) Tracings. During alignment, three-cell junctions (B) made up of Y-shaped interfaces (C) are converted to four-cell junctions (H) made up of X-shaped interfaces (I) by the elimination of an intervening contact. During this process, Myosin II (Sqh) is localized to long and shrinking contacts (D,J), Baz is localized to stable contacts (E,K) and Dlg is localized to long contacts (F,L).

of the *Drosophila* embryo, a subset of cells forms columns by aligning their AP edges (Fig. 7). This process initiates at specified boundaries and spreads across a limited cellular field, utilizing actomyosin contractility and polarity protein function. Although there are similarities with previously described tissue rearrangements, there are also striking differences that merit further study.

Junctional conversion

During alignment, three-cell junctions are converted to four-cell junctions by the elimination of a specific contact. This phenomenon has been observed in various epithelial tissues, such as during CE, in involuting tracheal placodes and developing wing cells (Bertet et al., 2004; Classen et al., 2005; Nishimura et al., 2007). Thus, junctional conversion is a common element in tissue remodeling. However, inspection of these cases also demonstrates that there are aspects unique to each.

During CE and tracheal placode involution, two three-cell junctions are converted to a four-cell junction by the elimination of a specific contact. However, this is not what drives the rearrangements that pattern these tissues. Rather, the resulting four-cell junction resolves further into two three-cell junctions through the growth of a new cell contact orthogonal to the original contact. This orthogonal regrowth is what drives the final cell rearrangements.

Three- to four-cell junction conversion also occurs among wing hair cells. This state also resolves, but in a manner distinct from that during CE. The four-cell junction resolves back to two three-cell junctions, but now in a random manner that maximizes cell contacts to assemble a hexagonally packed cell sheet (Classen et al., 2005). As in CE and tracheal placode involution, it is the last step, the re-establishment of three-cell junctions, that forms the final pattern.

The alignment among the denticle field cells contrasts with these cases. Here, it is the initial shift from three- to four-cell junctions that patterns the field. These cells make denticles, and a columnar alignment would be likely to optimize locomotion. To accomplish this, the underlying epithelial cells adopt a state far from equilibrium, as a polygonal array morphs into a rectilinear array of aligned cells. Junctional conversion is one step to accomplish this. We note that, eventually, cells along the columns tend to re-establish three-cell junctions with cells of neighboring columns, but in a manner that maintains columnar cell alignment. Presumably, once four-cell junctions are established, a secondary interaction, perhaps adhesion, becomes engaged along each column boundary to maintain alignment.

A general principle emerging from all these tissues is that the conversion from three- to four-cell junctions is central to patterning epithelia. However, there are key tissue-specific outcomes that often reflect whether and how a final re-establishment of junctions occurs. Thus, although there will be similarities between the mechanisms involved, there will also be significant differences. Currently, the analyses conducted differ in each of these cases, and so the comparisons remain incomplete.

Polarity proteins in cell alignment

There are some commonalities between polarity protein localizations among the above cases. During CE, Myosin II is enriched along shrinking contacts, whereas Baz is enriched along stable contacts (Bertet et al., 2004; Zallen and Wieschaus, 2004). During tracheal placode invagination, Myosin II is enriched along both contacts that shrink and some that do not, but there was no report of Baz localization (Nishimura et al., 2007). We show here that Baz and Dlg and the molecular motor Myosin II are enriched along specific boundaries during alignment. Crucially, both Dlg and Myosin II functionally assist in alignment. However, as is the case

for the tissues described above, two questions remain to be addressed: how are these proteins targeted to specific cellular interfaces, and how do they then mediate junctional conversion?

Considering the selection of interfaces within denticle field cells, perhaps a different polarity complex, potentially engaging in competitive exclusion to set up the enrichments, defines each contact. So far, we have not identified any candidates with compelling patterns. For instance, Crb was enriched generally among denticle field cells, but not at a specific interface, whereas aPKC was subtly enriched but only late in alignment, suggesting a subordinate role, if any. Since Baz defines the short, stable contact, whereas Dlg defines the long, stable contact, we might expect to identify a polarity protein that is enriched on the shrinking contact and can exclude both Baz and Dlg. One candidate is Par1, which phosphorylates and excludes Baz and Dlg from membranes in other contexts (Benton and Johnston, 2003; Zhang et al., 2007). Unfortunately, for many proteins, such as these, it has been difficult to deplete embryos of function without totally disrupting the epithelium.

Although it is a compelling idea, competitive exclusion is perhaps not a prime candidate for setting up or maintaining enrichments during alignment, as Baz enrichment was not altered in *dlg* mutants (Fig. 5). Similarly, during CE aPKC and Par6 are not required for Myosin II localization (Blankenship et al., 2006). In fact, during *C. elegans* gastrulation, PAR-3 and Myosin II actually co-localize to ingressing edges (Nance and Priess, 2002). It has been proposed that Myosin II can be templated by prior F-actin enrichment (Blankenship et al., 2006), but this too is not the case during alignment, where F-actin and Myosin become enriched at the same time.

Since junctional conversion is a recurring theme, the mechanism by which it occurs is of particular interest. During alignment and tracheal placode invagination, but not during CE, Myosin II is enriched both along contacts that are eliminated and stable contacts. Although we have shown that Myosin II is required for alignment, just how actomyosin contractility contributes to contact elimination, and how this process is counteracted along Myosin II-enriched stable contacts, are unknown. As during CE, a subtle enrichment on stable junctions is occasionally observed for DE-Cadherin and Armadillo (β-Catenin) (see Fig. S4J,N in the supplementary material). With regard to the shrinking contact, one possibility is that Myosin II pulls actin filaments past each other, collapsing the length of the contact (reviewed by Pilot and Lecuit, 2005), although how this might destabilize Cadherin-based adhesion is unknown. Another possibility is that actomyosin contractility might differentially affect endocytosis and exocytosis. When rates of endocytosis and exocytosis are balanced, interfaces are stably maintained. However, if the equilibrium is shifted towards endocytosis along a certain contact, for instance where contractility is increased (Pilot and Lecuit, 2005), that contact will shrink.

We found that Dlg is enriched along stable Myosin II-enriched contacts and we hypothesize that Dlg is involved in functionally distinguishing the two types of Myosin II-enriched contact. There are two ways in which Dlg could inhibit Myosin II function where they are co-enriched. First, Dlg might counteract Myosin II activity indirectly by facilitating exocytosis and membrane deposition as it has been suggested to do during cellularization (Lee et al., 2003). A bias towards deposition could lead to the apparent stabilization of contacts. Secondly, Dlg might recruit a Myosin II-inhibiting protein, such as Lgl, through one of its PDZ domains (Woods and Bryant, 1991).

Regardless of how Dlg counteracts Myosin II function, it was surprising that Dlg, a member of the basolateral group of epithelial polarity genes, influences cell-cell relationships apically in the epithelium at this stage. However, recent work has revealed that at about the stage when alignment begins, there is a transfer of basolateral responsibility from the Dlg group to the Yurt/Cora group (Laprise et al., 2009). That would free Dlg group genes to participate in other polarity events. With this in mind, we sought to test whether the basolateral protein Lgl, a negative regulator of Myosin II, would similarly be freed to assist Dlg in alignment (Peng et al., 2000). However, *lgl* germline clones have radically disrupted epithelia and zygotic mutants have persistent maternal contribution (Bilder et al., 2000; Peng et al., 2000).

Control and coordination of alignment

Convergent extension has some contribution from oriented cell divisions and some from junctional conversions (Bertet et al., 2004; Blankenship et al., 2006; da Silva and Vincent, 2007). Although oriented cell divisions contribute to CE more in the posterior portion of the embryo, junctional conversions occur for many cells with no spatially reproducible focus for initiation. By contrast, we have found that cell alignment differs between the prospective smooth and denticle fields, and, among denticle field cells, alignment begins along specific boundaries within each parasegment.

Among smooth field cells, stretching along the DV axis appears to be the major contributor to alignment. Even though Dlg makes some contribution to alignment here (Fig. 5F), it does not appear to be enriched on particular interfaces. However, stretching makes a minimal contribution to alignment among denticle field cells (Fig. 2C). This dramatic distinction between smooth and denticle field cells, coupled to our observation that specific cell columns initiate alignment events, strongly suggests the involvement of positional signals that are limited to, or emanate from, denticle field cells. In addition to starting at the 1/2 and 4/5 boundaries, alignment also initiates from the ventral midline and progresses laterally, eventually covering a third of the ectoderm (S.D. and R.P.S., unpublished). These observations raise the possibility that the 1/2 and 4/5 boundaries template the other boundaries by propagating a polarity signal from column to column. Candidate signals include Hedgehog signaling across the 1/2 boundary, Notch signaling across the 4/5 boundary and Egfr signaling across either boundary. Differential Egfr activation has been implicated in the conversion of three- to four-cell junctions in the tracheal placode (Nishimura et al., 2007), but how differential Egfr signaling translates into junctional conversion remains unknown.

Junctional conversion in other tissues

Four-cell junctions have been reported in several tissues (Nishimura et al., 2007; Sakurai et al., 2007). Their appearance during development might be a hallmark of cellular realignments integral to the patterning of that tissue. During development, signaling often occurs across smooth, defined boundaries, such as the DV compartment boundary in wing and segment boundaries in leg (de Celis et al., 1998; Major and Irvine, 2005; Sakurai et al., 2007). In fact, inspection of the data of Sakurai et al. shows that the tarsus/pretarsus boundary is composed of four-cell junctions that are strikingly reminiscent of those reported here (Sakurai et al., 2007).

A more closely studied example is the actomyosin enrichment along the boundary between the dorsal and ventral cells of the wing imaginal disk. Cells along this boundary form a smooth, lineage-restricted interface and do not intermix. The actomyosin 'fence' was implicated in maintaining this lineage-restricted signaling boundary (Major and Irvine, 2005; Major and Irvine, 2006). Notch signaling across the DV boundary enriches it for F-actin and Myosin II and

depletes it for Baz. Although a role for Baz was not tested, when Myosin II contractility is compromised, the integrity of the lineage-restricted boundary is disrupted. Under these conditions, the boundary is jagged and some cells can now mix. Our work would now suggest that the normal function of the actomyosin fence is to convert three- to four-cell junctions along the boundary. The failure of this would generate interdigitating cells, resulting in a non-aligned, jagged boundary, which would be the first step to cell mixing. By keeping cells aligned at the boundary, Myosin II activity might prevent them from interdigitating and support compartment integrity.

Acknowledgements
We thank Peter Bryant, Roger Karess, Dan Kiehart, Elisabeth Knust, Daniel St Johnston, Shoichiro Tsukita and the Bloomington Stock Center for mutant and transgenic flies; Andreas Wodarz and the Developmental Studies Hybridoma Bank for antibodies; Erfei Bi and the DiNardo and Ghabrial laboratories for thoughtful critique; and Andrea Stout for expert microscopy assistance. This work was funded by NIH R01 GM45747 (S.D.) and NIH Training Program in Developmental Biology 5T32HD007516 (R.P.S.). Deposited in PMC for release after 12 months.

Competing interests statement
The authors declare no competing financial interests.

Supplementary material
Supplementary material for this article is available at
http://dev.biologists.org/lookup/suppl/doi:10.1242/dev.048520/-/DC1

References

Adler, P. N. (2002). Planar signaling and morphogenesis in *Drosophila*. *Dev. Cell* **2**, 525-535.
Bachmann, A. and Knust, E. (1998). Dissection of cis-regulatory elements of the Drosophila gene Serrate. *Dev. Genes Evol.* **208**, 346-351.
Barros, C. S., Phelps, C. B. and Brand, A. H. (2003). *Drosophila* nonmuscle myosin ii promotes the asymmetric segregation of cell fate determinants by cortical exclusion rather than active transport. *Dev. Cell* **5**, 829-840.
Benton, R. and Johnston, D. S. (2003). *Drosophila* PAR-1 and 14-3-3 Inhibit Bazooka/PAR-3 to establish complementary cortical domains in polarized cells. *Cell* **115**, 691-704.
Bertet, C., Sulak, L. and Lecuit, T. (2004). Myosin-dependent junction remodelling controls planar cell intercalation and axis elongation. *Nature* **429**, 667-671.
Bertet, C., Rauzi, M. and Lecuit, T. (2009). Repression of Wasp by JAK/STAT signalling inhibits medial actomyosin network assembly and apical cell constriction in intercalating epithelial cells. *Development* **136**, 4199-4212.
Bilder, D., Li, M. and Perrimon, N. (2000). Cooperative regulation of cell polarity and growth by *Drosophila* tumor suppressors. *Science* **289**, 113-116.
Blankenship, J. T., Backovic, S. T., Sanny, J. S. P., Weitz, O. and Zallen, J. A. (2006). Multicellular rosette formation links planar cell polarity to tissue morphogenesis. *Dev. Cell* **11**, 459-470.
Classen, A.-K., Anderson, K. I., Marois, E. and Eaton, S. (2005). Hexagonal packing of *Drosophila* wing epithelial cells by the planar cell polarity pathway. *Dev. Cell* **9**, 805-817.
da Silva, S. M. and Vincent, J.-P. (2007). Oriented cell divisions in the extending germband of *Drosophila*. *Development* **134**, 3049-3054.
de Celis, J. F., Tyler, D. M., de Celis, J. and Bray, S. J. (1998). Notch signalling mediates segmentation of the *Drosophila* leg. *Development* **125**, 4617-4626.
Dickinson, W. J. and Thatcher, J. W. (1997). Morphogenesis of denticles and hairs in *Drosophila* embryos: involvement of actin-associated proteins that also affect adult structures. *Cell Motil. Cytoskeleton* **38**, 9-21.
Fernandez-Gonzalez, R., Simoes, S. D. M., Röper, J. C., Eaton, S. and Zallen, J. A. (2009). Myosin II dynamics are regulated by tension in intercalating cells. *Dev. Cell* **17**, 736-743.
Frank, L. H. and Rushlow, C. (1996). A group of genes required for maintenance of the amnioserosa tissue in *Drosophila*. *Development* **122**, 1343-1352.
Franke, J. D., Montague, R. A. and Kiehart, D. P. (2005). Nonmuscle myosin II generates forces that transmit tension and drive contraction in multiple tissues during dorsal closure. *Curr. Biol.* **15**, 2208-2221.
Hayashi, T. and Carthew, R. W. (2004). Surface mechanics mediate pattern formation in the developing retina. *Nature* **431**, 647-652.
Heisenberg, C.-P., Tada, M., Rauch, G.-J., Saude, L., Concha, M. L., Geisler, R., Stemple, D. L., Smith, J. C. and Wilson, S. W. (2000). Silberblick/Wnt11 mediates convergent extension movements during zebrafish gastrulation. *Nature* **405**, 76-81.
Hutterer, A., Betschinger, J., Petronczki, M. and Knoblich, J. A. (2004). Sequential roles of Cdc42, Par-6, aPKC, and Lgl in the establishment of epithelial polarity during *Drosophila* embryogenesis. *Dev. Cell* **6**, 845-854.
Irvine, K. D. and Wieschaus, E. (1994). Cell intercalation during *Drosophila* germband extension and its regulation by pair-rule segmentation genes. *Development* **120**, 827-841.
Jacinto, A., Wood, W., Woolner, S., Hiley, C., Turner, L., Wilson, C., Martinez-Arias, A. and Martin, P. (2002). Dynamic analysis of actin cable function during *Drosophila* dorsal closure. *Curr. Biol.* **12**, 1245-1250.
Keller, R. (2002). Shaping the vertebrate body plan by polarized embryonic cell movements. *Science* **298**, 1950-1954.
Kemphues, K. J., Priess, J. R., Morton, D. G. and Cheng, N. (1988). Identification of genes required for cytoplasmic localization in early *C. elegans* embryos. *Cell* **52**, 311-320.
Kiehart, D. P. and Feghali, R. (1986). Cytoplasmic myosin from *Drosophila melanogaster*. *J. Cell Biol.* **103**, 1517-1525.
Kiehart, D. P., Galbraith, C. G., Edwards, K. A., Rickoll, W. L. and Montague, R. A. (2000). Multiple forces contribute to cell sheet morphogenesis for dorsal closure in *Drosophila*. *J. Cell Biol.* **149**, 471-490.
Laprise, P., Lau, K. M., Harris, K. P., Silva-Gagliardi, N. F., Paul, S. M., Beronja, S., Beitel, G. J., McGlade, C. J. and Tepass, U. (2009). Yurt, Coracle, Neurexin IV and the Na^+,K^+-ATPase form a novel group of epithelial polarity proteins. *Nature* **459**, 1141-1145.
Lecuit, T. and Lenne, P.-F. (2007). Cell surface mechanics and the control of cell shape, tissue patterns and morphogenesis. *Nat. Rev. Mol. Cell Biol.* **8**, 633-644.
Lee, O.-K., Frese, K. K., James, J. S., Chadda, D., Chen, Z.-H., Javier, R. T. and Cho, K.-O. (2003). Discs-Large and Strabismus are functionally linked to plasma membrane formation. *Nat. Cell Biol.* **5**, 987-993.
Major, R. J. and Irvine, K. D. (2005). Influence of Notch on dorsoventral compartmentalization and actin organization in the *Drosophila* wing. *Development* **132**, 3823-3833.
Major, R. J. and Irvine, K. D. (2006). Localization and requirement for Myosin II at the dorsal-ventral compartment boundary of the *Drosophila* wing. *Dev. Dyn.* **235**, 3051-3058.
Martinez Arias, A. (1993). Development of *Drosophila melanogaster*. In *The Development of Drosophila melanogaster.* Cold Spring Harbor, NY: Cold Spring Harbor Laboratory Press.
McKenzie, E., Krupin, A. and Kelley, M. W. (2004). Cellular growth and rearrangement during the development of the mammalian organ of Corti. *Dev. Dyn.* **229**, 802-812.
Miller, K. G., Field, C. M. and Alberts, B. M. (1989). Actin-binding proteins from *Drosophila* embryos: a complex network of interacting proteins detected by F-actin affinity chromatography. *J. Cell Biol.* **109**, 2963-2975.
Nance, J. and Priess, J. R. (2002). Cell polarity and gastrulation in *C. elegans*. *Development* **129**, 387-397.
Nishimura, M., Inoue, Y. and Hayashi, S. (2007). A wave of EGFR signaling determines cell alignment and intercalation in the *Drosophila* tracheal placode. *Development* **134**, 4273-4282.
Nüsslein-Volhard, C., Wieschaus, E. and Kluding, H. (1984). Mutations affecting the pattern of the larval cuticle in *Drosophila melanogaster*. *Roux's Arch. Dev. Biol.* **193**, 267-282.
Oda, H. and Tsukita, S. (1999). Dynamic features of adherens junctions during Drosophila embryonic epithelial morphogenesis revealed by a D α-catenin-GFP fusion protein. *Dev. Genes Evol.* **209**, 218-225.
Peng, C.-Y., Manning, L., Albertson, R. and Doe, C. Q. (2000). The tumour-suppressor genes lgl and dlg regulate basal protein targeting in *Drosophila* neuroblasts. *Nature* **408**, 596-600.
Perrimon, N. (1988). The maternal effect of lethal(1)discs-large-1: a recessive oncogene of *Drosophila melanogaster*. *Dev. Biol.* **127**, 392-407.
Pilot, F. and Lecuit, T. (2005). Compartmentalized morphogenesis in epithelia: from cell to tissue shape. *Dev. Dyn.* **232**, 685-694.
Price, M. H., Roberts, D. M., McCartney, B. M., Jezuit, E. and Peifer, M. (2006). Cytoskeletal dynamics and cell signaling during planar polarity establishment in the *Drosophila* embryonic denticle. *J. Cell Sci.* **119**, 403-415.
Royou, A., Sullivan, W. and Karess, R. (2002). Cortical recruitment of nonmuscle myosin II in early syncytial *Drosophila* embryos: its role in nuclear axial expansion and its regulation by Cdc2 activity. *J. Cell Biol.* **158**, 127-137.
Sakurai, K. T., Kojima, T., Aigaki, T. and Hayashi, S. (2007). Differential control of cell affinity required for progression and refinement of cell boundary during *Drosophila* leg segmentation. *Dev. Biol.* **309**, 126-136.
Schock, F. and Perrimon, N. (2002). Cellular processes associated with germ band retraction in *Drosophila*. *Dev. Biol.* **248**, 29-39.
Tanentzapf, G. and Tepass, U. (2003). Interactions between the crumbs, lethal giant larvae and bazooka pathways in epithelial polarization. *Nat. Cell Biol.* **5**, 46-52.
Tilney, L. G. and Saunders, J. C. (1983). Actin filaments, stereocilia, and hair cells of the bird cochlea. I. Length, number, width, and distribution of stereocilia of each hair cell are related to the position of the hair cell on the cochlea. *J. Cell Biol.* **96**, 807-821.

van der Meer, S. (1977). Optical clean and permanent whole mount preparation for phase contrast microscopy of cuticular structures of insect larvae. *Drosoph. Inf. Serv.* **52**, 160-161.
Wallingford, J. B., Rowning, B. A., Vogeli, K. M., Rothbacher, U., Fraser, S. E. and Harland, R. M. (2000). Dishevelled controls cell polarity during *Xenopus* gastrulation. *Nature* **405**, 81-85.
Walters, J. W., Dilks, S. A. and DiNardo, S. (2006). Planar polarization of the denticle field in the *Drosophila* embryo: roles for Myosin II (Zipper) and Fringe. *Dev. Biol.* **297**, 323-339.
Wodarz, A., Hinz, U., Engelbert, M. and Knust, E. (1995). Expression of crumbs confers apical character on plasma membrane domains of ectodermal epithelia of *Drosophila*. *Cell* **82**, 67-76.
Wodarz, A., Ramrath, A., Kuchinke, U. and Knust, E. (1999). Bazooka provides an apical cue for Inscuteable localization in *Drosophila neuroblasts*. *Nature* **402**, 544-547.
Wong, K., Van Keymeulen, A. and Bourne, H. R. (2007). PDZRhoGEF and myosin II localize RhoA activity to the back of polarizing neutrophil-like cells. *J. Cell Biol.* **179**, 1141-1148.
Wong, L. L. and Adler, P. N. (1993). Tissue polarity genes of *Drosophila* regulate the subcellular location for prehair initiation in pupal wing cells. *J. Cell Biol.* **123**, 209-221.
Woods, D. F. and Bryant, P. J. (1989). Molecular cloning of the lethal(1)discs large-1 oncogene of *Drosophila*. *Dev. Biol.* **134**, 222-235.
Woods, D. F. and Bryant, P. J. (1991). The discs-large tumor suppressor gene of *Drosophila* encodes a guanylate kinase homolog localized at septate junctions. *Cell* **66**, 451-464.
Yamanaka, T., Horikoshi, Y., Sugiyama, Y., Ishiyama, C., Suzuki, A., Hirose, T., Iwamatsu, A., Shinohara, A. and Ohno, S. (2003). Mammalian Lgl forms a protein complex with PAR-6 and aPKC independently of PAR-3 to regulate epithelial cell polarity. *Curr. Biol.* **13**, 734-743.
Zallen, J. A. and Wieschaus, E. (2004). Patterned gene expression directs bipolar planar polarity in *Drosophila*. *Dev. Cell* **6**, 343-355.
Zhang, Y., Guo, H., Kwan, H., Wang, J.-W., Kosek, J. and Lu, B. (2007). PAR-1 kinase phosphorylates Dlg and regulates its postsynaptic targeting at the *Drosophila* neuromuscular junction. *Neuron* **53**, 201-215.